Pion scattering and electro-production on nucleons in the resonance region in chiral quark models

Simon Širca^{1,ab}, Bojan Golli^{cb}, Manuel Fiolhais^d, and Pedro Alberto^d

^aFaculty of Mathematics and Physics, University of Ljubljana, Slovenia

^bJožef Stefan Institute, Ljubljana, Slovenia

^cFaculty of Education, University of Ljubljana, Slovenia

^dDepartamento de Fisica and Centro de Fisica Computacional, Universidade de Coimbra, Portugal

Pion scattering and electro-production amplitudes have been computed in a coupled-channel framework incorporating quasi-bound quark-model states, based on the Cloudy Bag model. All relevant low-lying nucleon resonances in the P33, P11, and S11 partial waves have been covered, including the $\Delta(1232)$, the $N^*(1440)$, $N^*(1535)$, and $N^*(1650)$. Consistent results have been obtained for elastic and inelastic scattering (two-pion, eta-N, and K-Lambda channels), as well as for electro-production. The meson cloud has been shown to play a major role, in particular in electro-magnetic observables in the P33 and P11 channels.

The study of pion scattering and electro-production on nucleons in the region of low-lying resonances helps us establish meaningful connections between the data and resonance properties obtained in model calculations. One of the key aspects is the interplay of quark and meson degrees of freedom. The conceptual foundations of our approach in chiral quark models date back to the paper [1], in which we demonstrated the importance of the pion cloud in the electro-production of pions in the region of the $\Delta(1232)$. We found that the pion cloud contributes $\sim 45\,\%$ to the magnetic dipole amplitude, and strongly dominates the electric quadrupole amplitude, a result later confirmed by many related calculations.

In our previous work [2] we have shown that in models in which mesons couple linearly to the quark core, the elements of the K matrix for meson-baryon scattering $MB \to M'B'$ in the basis with good total angular momentum J, isospin T and parity take the form:

(1)
$$K_{M'B'MB}^{JT} = -\pi \mathcal{N}_{MB} \langle \Psi_{JT}^{MB} || V_{M'}(k) || \Psi_{B'} \rangle, \qquad \mathcal{N}_{MB} = \sqrt{\frac{\omega_M E_B}{k_M W}}.$$

Here $|\Psi_{IT}^{MB}\rangle$ is the principal value state:

$$|\Psi_{JT}^{MB}\rangle = \mathcal{N}_{MB} \left\{ [a^{\dagger}(k_M)|\Psi_B\rangle]^{JT} + \sum_{\mathcal{R}} c_{\mathcal{R}}^{MB} |\Phi_{\mathcal{R}}\rangle + \sum_{M'B'} \int \frac{\mathrm{d}k \, \chi^{M'B'\,MB}(k)}{\omega_k + E_{B'}(k) - W} \left[a^{\dagger}(k) |\Psi_{B'}\rangle \right]^{JT} \right\} ,$$

¹simon.sirca@fmf.uni-lj.si

 $\Psi_{B'}$ is the fully dressed outgoing baryon state, and $V_{M'}(k)$ is the quark-meson vertex determined in the underlying quark model. The first term represents the free meson $(\pi, \eta, \sigma, ...)$ and the baryon $(N, \Delta, ...)$ and defines the channel, the next term is the sum over *bare* tree-quark states $\Phi_{\mathcal{R}}$ involving different excitations of the quark core, the third term introduces meson clouds around different isobars. In the case of two-pion decays, we assume that they proceed either through an unstable meson (e.g. ρ -meson, σ -meson) or through a baryon resonance (e.g. $\Delta(1232)$, $N^*(1440)$). The meson amplitudes $\chi^{M'B'MB}(k)$ are proportional to the (half) off-shell K-matrix elements (1), and obey a coupled set of equations of the Lippmann-Schwinger type. The resulting amplitudes take the form

$$\chi^{M'B'MB}(k) = -\sum_{\mathcal{R}} c_{\mathcal{R}}^{MB} \mathcal{V}_{B'\mathcal{R}}^{M'}(k) + \mathcal{D}^{M'B'MB}(k) ,$$

where the first term represents the contribution of resonances, while $\mathcal{D}^{M'B'}MB(k)$ originates in non-resonant background processes. Here $c_{\mathcal{R}}^{MB} = \mathcal{V}_{B\mathcal{R}}^{M}/(Z_{\mathcal{R}}(W)(W-M_{\mathcal{R}}))$, $\mathcal{V}_{B\mathcal{R}}^{M}$ is the dressed matrix element of the quark-meson interaction between the resonant state and the baryon state in the channel MB, and $Z_{\mathcal{R}}$ is the wave-function normalization. The resulting physical resonant states \mathcal{R} are superpositions of the bare 3-quark states $\Phi_{\mathcal{R}'}$. The T matrix is obtained by solving the Heitler's equation T = K + iTK.

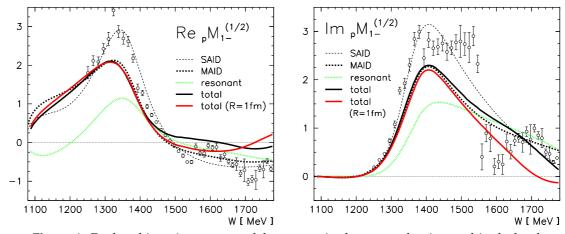


Figure 1: Real and imaginary parts of the magnetic electro-production multipole for the proton target, isospin-1/2 channel, in the P11 partial wave (the Roper resonance).

More recently, we have extended the method outlined above to the calculation of meson electro-production amplitudes by including the γN channel [3,4]. The electro-production amplitude in the vicinity of a chosen resonance $\mathcal{R}=N^*$ can be cast in the form

$$\mathcal{M}_{\gamma NMB} = \mathcal{M}_{\gamma NMB}^{(res)} + \mathcal{M}_{\gamma NMB}^{(bg)} = \sqrt{rac{\omega_{\gamma} E_N^{\gamma}}{\omega_M E_B}} rac{1}{\pi \mathcal{V}_{RN^*}} \langle \Psi_{N^*}^{(res)}(W) | V_{\gamma} | \Psi_N
angle \, T_{MBMB} + \mathcal{M}_{\gamma NMB}^{(bg)} \, ,$$

where T_{MBMB} is the meson-baryon scattering amplitude, and the electro-excitation of the resonance is described by the helicity amplitude $\langle \Psi_{N^*}^{(res)}(W)|V_{\gamma}|\Psi_N\rangle = A_{\gamma N \to N^*}$. Here

 $V_{\gamma}(\mu, \vec{k}_{\gamma})$ is the interaction of the photon with the electro-magnetic current, and contains quark and pion contributions as specified by the underlying quark model.

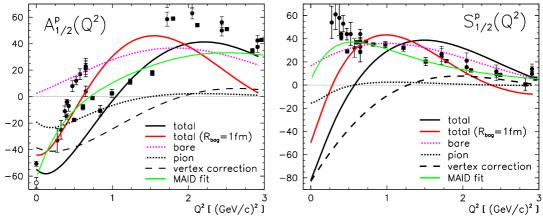


Figure 2: Different contributions to the transverse and scalar helicity amplitudes for the electro-excitation of the $N^*(1440)$ (Roper) resonance in the P11 partial wave.

In the P11 case we have included the πN , $\pi \Delta$, $\pi N^*(1440)$ and σN channels, while the sum over $\mathcal R$ consists of the nucleon, $N^*(1440)$, and $N^*(1710)$ resonance; in the S11 case we have considered the πN , $\pi \Delta$, $\pi N^*(1440)$, ρN and $K \Delta$ channels, as well as $N^*(1535)$ and $N^*(1650)$ resonances. We have used the quark-model wave-functions for the negative-parity states in the form $\Phi_{\mathcal R} = c_A^{\mathcal R} |(1s)^2 (1p_{3/2})^1 \rangle + c_P^{\mathcal R} |(1s)^2 (1p_{1/2})^1 \rangle_1 + c_{P'}^{\mathcal R} |(1s)^2 (1p_{1/2})^1 \rangle_2$, where the mixing coefficients of [5] have been adopted.

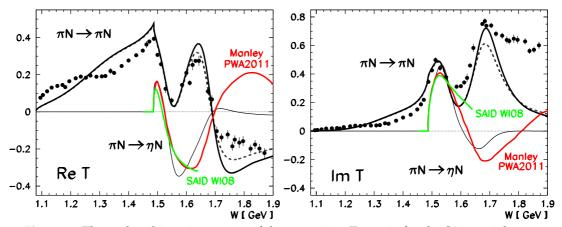


Figure 3: The real and imaginary part of the scattering T matrix for the S11 partial wave. Shown are the elastic results as well as those for the $\pi N \to \eta N$ channel. The solid lines were obtained by using the reduced value of the d-wave $\pi \Delta$ coupling while the dashed lines correspond to the unmodified quark-model values for the baryon-meson couplings.

The quark-meson vertices were computed in a SU(3)-extended Cloudy Bag Model with the quark-meson Lagrangian $\mathcal{L}_{CBM}^{(qM)} = -(\mathrm{i}/2f_M)\,\overline{q}\gamma_5\lambda_a q\phi_a\delta\,(r-R_{bag})$, $a=1,2,\ldots,8$. We used $R_{bag}=0.83$ fm, the interaction parameter $f_\pi=76$ MeV which reproduces the experimental $g_{\pi NN}$ coupling, $f_K=1.2\,f_\pi$, and either $f_\eta=1.2\,f_\pi$ or $f_\eta=f_\pi$. The bare masses of $\Phi_\mathcal{R}$ were adjusted to reproduce the positions of the resonances.

We have reproduced reasonably well the main features of the M_{1-} electro-production amplitude from the threshold up to $W \sim 1700$ MeV (Figs. 1 and 3), as well as the transverse and scalar helicity amplitudes for Q^2 up to $\sim 3~{\rm GeV^2/c^2}$. Our calculations indicate that the pion cloud plays an important role, especially in the region of low Q^2 (long-range effects). In the case of the $N^*(1440)$ resonance (Fig. 2), the quark contribution to $A_{1/2}^p$ is positive, while the pion contribution and the vertex corrections due to meson loops are negative. These two effects are responsible for the zero crossing of the amplitude. At higher Q^2 (short-range physics) the quark core takes over, rendering $A_{1/2}^p$ positive.

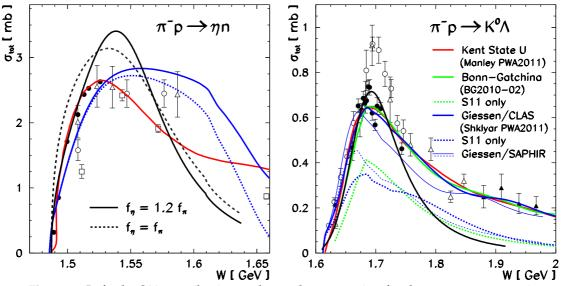


Figure 4: Left: the S11 contribution to the total cross-section for the $\pi^- p \to \eta n$ reaction. Right: total cross-section for the $\pi^- p \to K^0 \Lambda$ process. Our result: black solid and dashed lines; other analyses are color-coded in the figure legend.

The results for pion-induced meson production amplitudes in the S11 partial wave are shown in Fig. 3. Near the $N^*(1535)$ resonance, just above the η threshold, the elastic and inelastic amplitudes are strongly influenced by the s-wave ηN channel. Near the $N^*(1650)$ resonance, additional channels become more relevant, such as the $\pi\Delta$ with l=2, the $K\Lambda$ with l=0, two channels involving the ρ meson with l=0 ($\rho_1 N$) and l=2 ($\rho_3 N$), and the $\pi N^*(1440)$ channel with l=0. The S11 contributions to the total cross-section for the $\pi^- p \to \eta n$ and $\pi^- p \to K^0 \Lambda$ processes are shown in Fig. 4 (left and right, respectively).

The results for η photoproduction are shown in Fig. 5 (left). The behavior is almost completely driven by the properties of the $N^*(1535)$ resonance and the threshold behavior of the ηN amplitude, but is almost insensitive to background processes. The good overall agreement with the data for η production strongly supports our conjecture about the dominance of the genuine three-quark configuration in the $N^*(1535)$ state. The absolute value of the E_{0+} amplitude in the $K\Lambda$ channel is shown in Fig. 5 (right). While the cross-section for pion-induced production of K^+ appears to be over-estimated in our model, the photoproduction amplitude is smaller than predicted by phenomenological analyses. This discrepancy remains an open question and represents a challenge for further investigation.

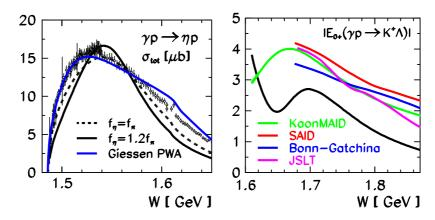


Figure 5: Left: total cross-section for eta photoproduction on the proton. Right: the absolute value of the transverse K^+ photo-production amplitude E_{0+} . Our result: black solid and dashed lines; other calculations are color-coded in the figure legend.

Acknowledgement The Authors wish to thank Andrei Sarantsev and Vitaliy Shklyar for providing us with the most recent data files from their analyses.

References

- [1] M. Fiolhais, B. Golli, S. Širca, Phys. Lett. B 373 (1996) 229.
- [2] B. Golli, S. Širca, Eur. Phys. J. A 38 (2008) 271.
- [3] B. Golli, S. Širca, M. Fiolhais, Eur. Phys. J. A 42 (2009) 185.
- [4] B. Golli, S. Širca, Eur. Phys. J. A 47 (2011) 61.
- [5] F. Myhrer, J. Wroldsen, Z. Phys. C 25 (1984) 281.